inter.noise
HAMBURG 2016

A 3D envelopment procedure for tyre belt radiated noise level prediction

Philippe KLEIN[1]; Julien CESBRON[2]

[1] IFSTTAR, AME, LAE, Université de Lyon/CeLyA, France

[2] IFSTTAR, AME, LAE, LUNAM Université, France

ABSTRACT

The HyRoNE model is based on a "hybrid" approach that combines simplified physical models and statistical relationships built upon a database for the prediction of rolling noise levels. 2D enveloped texture profiles, intended to account for the partial tyre/road contact, are used in the current version for predicting the noise levels due to the tyre belt vibration.

Smooth road surfaces in the database highlight contributions in the low and medium frequency domain not related to the enveloped road texture and suggest to also considering the tyre tread pattern for the tyre belt radiated noise level prediction. Due to the essentially different road and tyre tread roughness, 2D profiles are no longer suitable and therefore a 3D envelopment procedure is proposed to account for a combined road and tyre roughness.

This 3D procedure is tested on a database which includes 3D texture and noise measurements performed on a set of impervious road surfaces within the DEUFRAKO project ODSurf. Noise measurements with a patterned tyre are considered. The results are compared with those obtained with the 2D envelopment procedure.

Keywords: Tyre/road noise, Road texture, Tread pattern, Envelopment, Hybrid model, Noise level prediction
I-INCE Classification of Subjects Number(s): 11.7.1

1. INTRODUCTION

The road texture is acknowledged to have a significant influence on rolling noise for tyres with not too aggressive tread pattern. Empirical relationships between road texture and rolling noise have been pointed out a long time ago (1) that qualitatively show the influence of the road texture with associated dominant generation mechanisms depending on the frequency range considered.

"Hybrid" models are intended to quantitatively improve the prediction of rolling noise with respect to empirical relationships from the road and tyre characteristics. They are based on a combination of simplified physical models and statistical relationships tuned upon a road surface database containing rolling noise related quantities and road and tyre parameters.

The HyRoNE model uses the "enveloped" texture to account for the partial tyre/road contact for the prediction of the noise generated by the tyre belt vibration. The present version uses the texture information as 2D profiles measured in the rolling direction. It has been previously constructed and validated on conventional road surfaces with quite satisfactory results. The lack of transverse texture information prevents to construct a model valid for all type of surfaces and to introduce the tyre tread pattern that may greatly influence the noise generated, especially on rather smooth surfaces.

In this study, the model has therefore been improved with 3D texture data. A new envelopment procedure has been developed for handling 3D road texture data as well as the tyre tread pattern. Based on these improvements, a 3D version of HyRoNE model has been tested. The data used to test the model have been collected within the DEUFRAKO ODSURF project. This database is presented in section 2. As a reference method, the 2D version of HyRoNE model has been reconstructed with these data and is described in section 3. Section 4 deals with the contact model used to implement the new 3D envelopment procedure, which results are described in section 5. Finally, section 6 deals with the

[1] philippe.klein@ifsttar.fr
[2] julien.cesbron@ifsttar.fr

fitting of the new version of HyRoNE model based on the 3D envelopment procedure.

2. ODSURF ROAD SURFACE DATABASE

Several road surfaces have been measured within the framework of the DEUFRAKO ODSURF project. The test sites are located in France and in Germany. Most of the measurements have been performed on test tracks. The first one is the Ifsttar reference test track located in Bouguenais (France) and the second one is a BASt test track located in Geilenkirchen (Germany). Additional measurements have been performed on two trafficked roads in France (2) and on a rest area closed to traffic in Germany. Overall, 20 road surfaces have been tested: 16 surfaces with random texture (absorbing and non-absorbing surfaces), 3 deterministic surfaces (a slick resin, a longitudinally grooved surface, a slick surface with cylindrical holes) and a pseudo-randomly grooved Ultra High Performance Concrete. Texture and noise measurements have been performed together on 19 of these surfaces (all but the slick resin). Absorption measurements were performed on 7 of them considered as absorbing or likely absorbing road surfaces. More details can be found in (3).

2.1 Tyre/Road Noise and Sound Absorption Measurements

The Close-Proximity (CPX) and the Coast-By (CB) measurement methods have been used simultaneously to characterize tyre/road noise over 20 meters of each road section, following the recommendations of the CPX French method and the EU Directive 2001/43/EC respectively. The transmission of the test vehicle was put in neutral gear just before entering the 20 m section to be characterized. The average speed for each run was obtained from the CPX measurement. Several runs were performed for different speeds with a 5 km/h interval. The speed limits were chosen depending on the configuration of the test site. On Ifsttar and BASt test sites, the noise measurements were performed at least from 65 km/h to 110 km/h. It was not possible to reach such high speeds in some cases, for which the upper speed was limited to 90 km/h or even 70 km/h.

The test vehicle was a passenger car Renault Scenic (Figure 1, left). The vehicle was fitted with patterned Michelin Energy E3A 195/60R15 tyres on the one hand, and with slick Avon 210/60R16 racing tyres on the other hand. The results obtained with the slick tyres are not presented in this paper.

Figure 1 – Left: Test vehicle and tyres – Right: absorption measurement system

For each road surface, the measured noise levels as a function of logarithm of vehicle speed were analyzed by means of a linear regression method. On the one hand, it provides LAmax values and associated third-octave pass-by levels at reference speeds. On the other hand, LAeq CPX values and associated third-octave CPX noise levels are similarly obtained.

For acoustically absorbing or possibly absorbing road surfaces, sound absorption was measured in normal incidence according to ISO 13472-1. The measurement system can be seen in Figure 1 (right).

2.2 3D Texture Measurements

The texture measurements have been performed with a newly developed equipment based on a 2D laser sensor moved above the surface by a motorized linear axis allowing the acquisition of 3D texture samples as 5 cm wide and 1.50 m long longitudinal stripes (Figure 2). The lateral position of each stripe is controlled by a transverse positioning table. For each position of the equipment eight parallel overlapping stripes are used to reconstruct a full texture map of size 0.35 m wide and 1.50m long.

Figure 2 – 3D texture measurement system

For each pavement, two to four full texture maps have been measured with a 10cm long overlapping zone enabling the connection between adjacent maps. A stretched wire was used for ensuring a good alignment of successive positions of the chassis. Texture maps with dimensions of about 0.35 m wide and 2,90m to 5,70m long have been reconstructed. These measurements have been performed in the CPX measurement wheel path and centered on the CB measurement microphone position.

The raw and "enveloped" third-octave texture spectra which are used in the models described in the following sections are evaluated according to the recommendations of ISO 13473-4.

2.3 Road Surfaces Used for Model Fitting

In the present paper, the absorbing road surfaces are not considered to avoid possible biases due to porosity and absorption effects. Road pavements that may induce typical air resonance mechanisms (such as the longitudinally grooved surface or the slick surface with cylindrical cavities) are not taken into account too. Finally, 11 road pavements are considered in the following analysis. They are listed in Table 1.

Table 1 – Road surfaces considered in the study

Name	Type	Grain size [mm]	Test site
A'	Surface Dressing	8/10	Ifsttar
E1	Dense Asphalt Concrete	0/10	Ifsttar
E2	Dense Asphalt Concrete	0/10	Ifsttar
G0	Flexible Dense Asphalt Concrete	0/10	Ifsttar
ISO	Dense Asphalt Concrete (ISO 10844)	0/8	Ifsttar
L2	Sand Asphalt	0/4	Ifsttar
LOA	Noise Optimized Asphalt Concrete	-	BASt
LS1	Stone Mastic Asphalt	0/8	BASt
M1	Very Thin Asphalt Concrete (type 1)	0/2-6/10	Ifsttar
PMA	Porous Mastic Asphalt	-	BASt
PMAG	PMA with rubber granulates	-	BASt

3. FITTING OF HyRoNE 2D VERSION

3.1 HyRoNE Description

The HyRoNE model (4,5,6) predicts the pass-by tyre/road noise of a passenger car depending on the road surface characteristics. The prediction process distinguishes two frequency domains: the low and medium frequency range where tyre/road noise is mainly attributed to the radiation of the tyre belt, and the high frequency domain where tyre/road noise is mainly attributed to air-pumping. The transition frequency (also called cross-over frequency in (7)) is the limit between both domains. Third-octave noise levels between 100 Hz and 5 kHz are predicted from third-octave raw or "enveloped" texture levels at wavelength $\lambda_i = V / f_i$, where V is the rolling speed and f_i the third-octave noise frequency.

The enveloped texture is used in the low and medium frequency range to account for the possible partial contact between the road surface and the tyre belt. It is based on a 2D static contact model between the road profile and an elastic half-space (8). The problem to be solved is made periodic to avoid edge effects. The sketch of the envelopment is shown Figure 3. In the high frequency range, the raw texture is used for taking the possible overpressure release within the contact zone into account.

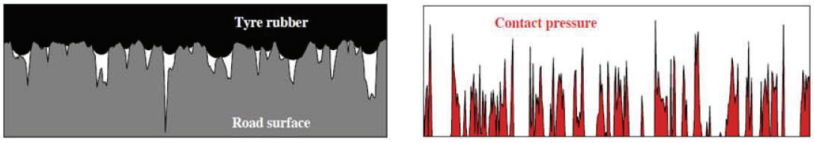

Figure 3 – The 2D envelopment procedure

The third-octave band noise levels L_i at frequencies f_i induced by texture are given by:

$$\begin{aligned} L_i &= a_i + b_i\, L_{eTi} \quad , \quad f_i \le f_t \\ L_i &= a_i + b_i\, L_{Ti} \quad , \quad f_i > f_t \end{aligned} \tag{1}$$

where L_{eTi} and L_{Ti} stand respectively for the enveloped and raw third-octave band texture levels at wavelength λ_i, a_i and b_i are the offset and the slope of the linear statistical relationships, and f_t is the transition frequency.

The correction for a possible acoustic absorption of the road surface is introduced as an excess attenuation ΔL_{pi} with respect to a perfectly reflecting road surface, with the tyre/road noise source considered on the ground and omnidirectional. The global level predicted by the HyRoNE model is thus given by:

$$L_g^{(T)} = 10 \log\left(\sum_i 10^{(L_i + \Delta L_{pi})/10} \right) \tag{2}$$

Every vehicle/tyre/speed configuration requires a specific construction of the prediction tool, i.e. the determination of the optimal rubber Young's modulus value E, the transition frequency f_t and the statistical relationship coefficients a_i and b_i. This determination is performed by minimizing the error between measured and predicted global noise levels averaged over the dataset.

3.2 Global Noise Level Prediction

The construction of the HyRoNE model within the DEUFRAKO project P2RN had been previously carried out for the patterned Michelin Energy E3A tyres fitted on the Renault Scenic (5). The texture data was measured as 2D profiles. The construction was carried out for several reference speeds taking into account dense as well as acoustically absorbent road surfaces. For the speed of 90 km/h, the transition frequency was determined to be 1250 Hz, and the value of the optimal envelopment parameter was $E = 6$ MPa.

Within the ODSurf project the model fitting was carried out for the same tyre with the data collected on the dense or poorly absorbing road surfaces listed in Table 1. However, unlike within the P2RN project, the dataset used here comprises a rather smooth surface (the ISO surface).

The model was calibrated for the speed of 90 km/h for predicting CB global noise levels. The optimal E value was determined to be 3 MPa, without taking into account the ISO surface. The same transition frequency was identified as within the P2RN project, namely 1250 Hz.

The correspondence between predicted and measured global CB levels reconstructed from the third-octave band levels is given Figure 4. The graph on the left is the correspondence obtained without considering the ISO surface in the model construction. The graph on the right is obtained with all surfaces. The black solid lines is the regression line estimated between predicted and measured levels for the surfaces used in the construction and the dashed black lines stand for the perfect measurement/prediction match. The average prediction error in the first case amounts to 0.6 dBA. However the prediction error for the ISO surface is very large. It is 3.4 dBA. In the second case, the mean prediction error is higher and amounts to 1.0 dBA. The global CB levels of the roughest (A') and smoothest (ISO) road surfaces are both underestimated by almost 2 dBA.

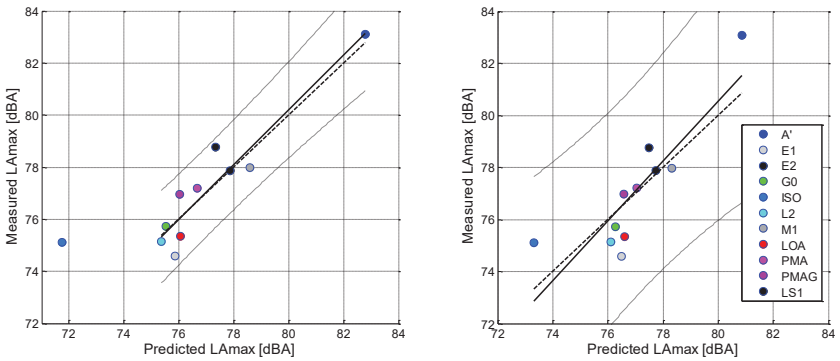

Figure 4 – Relationship between predicted and measured LAmax at 90 km/h reconstructed from third-octave

CB noise levels for the E3A tyre – Left: all but the ISO surfaces considered – Right: all surfaces considered

3.3 Trends for Smooth Road Surfaces

The graph in Figure 5 illustrates an identified cause explaining that the overall correspondence between measured and predicted levels deteriorates when the smooth ISO surface is taken into account. This figure gives the evolution of noise levels in the 500 Hz third-octave band as a function to the 2D enveloped texture levels for the 11 conventional surfaces considered. It can be observed that the ISO road surface causes a slight inflection of the texture/noise relationship in the range of low enveloped texture levels. It is easy to construct from these data a simple model with two incoherent contributions: one constant contribution not related to the enveloped texture (represented by the horizontal dotted line), another contribution which depends linearly from the enveloped texture levels (diagonal dotted line). The energetic sum of both contributions is represented by the black curve that fits quite well to the measurement points. Similar observations can be found in (9). It is to be noted that the slope of the diagonal line is very close to 1. Several reasons can be given to explain this behavior on low-roughness surfaces. The contribution independent of the enveloped texture may be due to air pumping phenomena known as amplified on smooth surfaces. It may also be partly due to the contribution of the tyre tread blocks that combine with the road surface to produce vibrational noise levels higher than expected from the road texture alone.

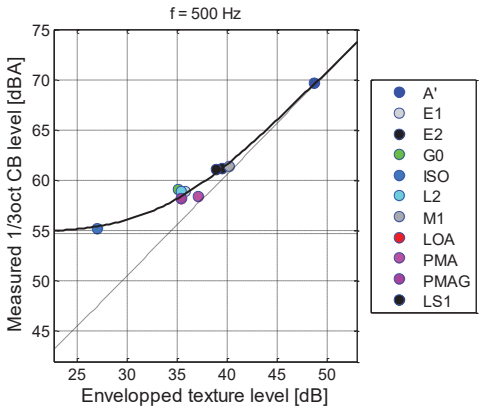

Figure 5 – Relationship between third-octave levels at 500 Hz and 90 km/h and enveloped texture levels

This simple model improves the noise prediction for frequencies up to 800 Hz or 1 kHz but does not provide the mechanism at stake in this frequency range on smooth road surfaces. To be able to separate the noise contributions due to the tyre belt vibration and to air-pumping sources, uncertainties about the mechanism affecting this behavior on low-roughness surfaces should be overcome by developing a method to account for the combined tyre/road roughness influence on the noise radiated by the tyre belt. Several approaches are possible for that purpose. Contact forces used for instance in the SPERoN model (5,6) or given by the multi-asperity contact model (10) are possibilities. In the remainder of this paper, a solution based on a 3D envelopment procedure is proposed.

4. 3D STATIC CONTACT MODEL

4.1 Non-periodic Contact Model

A semi-infinite elastic half-space characterized by its Young's modulus E and Poisson's ratio ν is considered to model the tyre tread. A rigid body is applied on this elastic half-space with a given normal load or uniform pressure P_0. A pressure distribution $p(x,y)$ is generated at the parts in contact C. The corresponding deflection of the elastic body is given by the Boussinesq's formula:

$$w(x,y) = \iint_C p(u,v)g(x,y;u,v)dudv \quad \text{where} \quad g(x,y;u,v) = \frac{1-\nu^2}{\pi E}\frac{1}{\sqrt{(x-u)^2+(y-v)^2}} \tag{3}$$

The global equilibrium condition is written as:

$$\iint_C p(x,y)dxdy = F \tag{4}$$

In the case of a rectangular domain, this problem can be discretized in a rectangular grid and solved using an iterative algorithm to find the contact zone C, the contact pressure p and the half-space surface displacement w.

4.2 Periodic Contact Model

The same problem as described in Section 4.1 is addressed but it is now considered to be periodic. This means that the rectangular domain considered above is infinitely repeated in the x and/or y directions. This is performed to avoid edge effects that may appear at the limits of the rectangular domain yielding to high overpressures at the edges and lower averaged pressure in the middle of the domain (see similar observations for the 2D case in (8)).

The periodic problem comes down to consider the infinite repetition of the rectangular domain considered, in one direction (x or y) for a semi-periodic problem, in two directions (x and y) for a fully periodic contact problem. The Green's function for the (semi-)periodic problem is obtained by evaluating the infinite sum of the shifted contributions of the Green's function of the non-periodic case $g(x,y;u,v)$. A scheme for the evaluation of the Green's function is given Figure 6. The red arrow stands for a unitary normal load applied on the rectangular domain considered. For a semi-periodic problem, unitary loads represented by arrows in blue are also to be considered. For a fully periodic problem, all the unitary loads are to be considered.

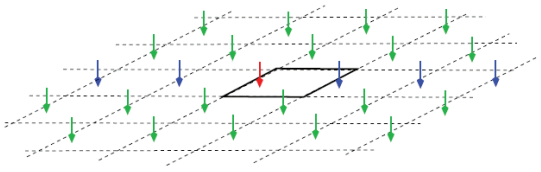

Figure 6 – Scheme for the evaluation of the Green's function for the periodic contact problems

In this case, the relative displacement of the frontier of the elastic half-space with respect to the displacement at a given point (x_0,y_0), due to a pressure distribution $p(x,y)$, is expressed as:

$$w(x,y)-w(x_0,y_0)=\iint_C \left[G(x,y;u,v)-G(x_0,y_0;u,v)\right]p(u,v)dudv \tag{5}$$

For a semi-periodic problem in direction x and a fully periodic problem, the Green's function writes respectively (L_x and L_y are the length and width of the rectangular domain considered):

$$G(x,y;u,v)=\sum_{n=-\infty}^{+\infty} g(x,y;u-nL_x,v) \tag{6}$$

$$G(x,y;u,v)=\sum_{n=-\infty}^{+\infty}\sum_{m=-\infty}^{+\infty} g(x,y;u-nL_x,v-mL_y) \tag{7}$$

The global equilibrium of the system is written as:

$$\frac{1}{L_xL_y}\int_0^{L_x}\int_0^{L_y} p(x,y)dxdy = P_0 \tag{8}$$

Illustrations of edge effects encountered with a rigid flat punch in the non-periodic, semi-periodic and fully periodic cases are given Figure 7. The rectangular domain is discretized in 20x100 square elements. The edge effects clearly disappear, laterally in the semi-periodic case and completely in the fully periodic case. Practically, with the formulation described above, the edge effect is not completely removed. The infinite sums in equations (6) and (7) cannot be numerically infinite and are truncated. The maximum values of summation indexes n and m are chosen such as to sufficiently limit the edge effect. For the fully periodic case for instance, the maximum deviation at the edges with respect to the prescribed constant pressure is obtained for $|n,m| \leq 50$. The deviation is less than 1% and it is of

course not visible in the graph.

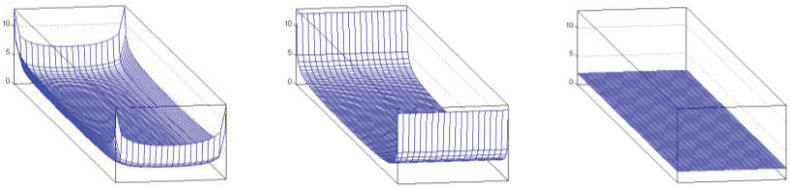

Figure 7 – Numerically evaluated contact pressure for a rigid flat punch - Left: non periodic – Middle: semi-periodic – Right: periodic in both directions

4.3 Equivalence between 2D and 3D Enveloped Profiles

The first motivation to build a 3D envelopment method is that the 2D and 3D envelopments are not equivalent. The method of 2D envelopment comes down to considering the road texture as a 2D corrugated surface instead of an isotropic one. To highlight this, 2D and 3D envelopments were calculated on several surfaces and compared in terms of enveloped texture spectra.

The adopted approach for the 2D/3D comparison is to extract from the tested surfaces rectangular parts of 25 mm wide and 0.5 m long (the sampling interval used here amounts to 0.8 mm). For each extracted surface part, a 2D envelopment is performed on the median longitudinal profile. A 3D fully periodic envelopment is also performed, from which the median longitudinal enveloped profile is extracted. An example of 3D periodic envelopment is shown in Figure 8.

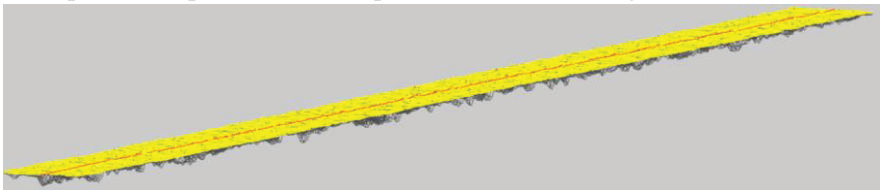

Figure 8 – Example of 3D periodic envelopment performed on a 25 mm by 500 mm surface – In gray: raw texture – In yellow: enveloped surface – In red: median profile for comparison with 2D enveloped profile

The 2D enveloped texture spectrum obtained for each surface with a Young's modulus value chosen equal to 6 MPa are used as references for the comparison. 3D enveloped profile spectra are evaluated for 8 Young's modulus values ranging from 1 MPa to 5 MPa with a geometric progression. The differences between the 3D enveloped texture levels and the 2D reference are drawn Figure 9 for 4 road surfaces with very different textures (A', A, E2 and ISO) for wavelengths ranging from 8 mm to 250 mm. First, it can be observed that, whatever the road surface considered, the value of E for which 2D and 3D levels are equal depends on the texture wavelength. The smaller the wavelength, the greater the E value for which equality is reached. Second, for one wavelength considered, the value of E for which 2D and 3D enveloped levels are equal changes depending on the road surface. Therefore there is no equivalence between 2D and 3D envelopments in terms of texture spectra.

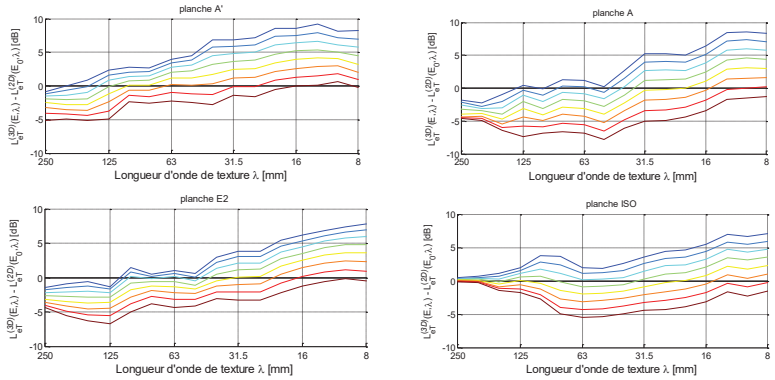

Figure 9 – Differences between 3D and 2D enveloped texture spectra for several values of E ranging from 1 MPa (brown curves) to 5 MPa (blue curves)

It can also be concluded that it would be difficult to find a 2D envelopment parameter value for enveloping a (strongly anisotropic) tyre tread that would be equivalent to the optimal value identified

for isotropic road surfaces. Therefore, the combination of tyre and road roughness cannot be achieved from 2D information.

5. 3D ENVELOPMENT FOR NOISE PREDICTION

5.1 Input Data

The input for the 3D envelopment calculation is the 3D combined tyre/road roughness. It is obtained by subtracting the developed tyre tread height from the road texture height. In this way, the tyre overall transverse shape and tread grooves are transferred to the road texture. Since the road samples are longer than a tyre revolution, the tread band is repeated as necessary. The contact is thus evaluated between the rigid tyre/road roughness and a flat elastic half-space. An illustration is given Figure 10. Three maps of 23 cm wide and 1 m long are drawn. The map at the top (left) gives an extract of the developed tyre tread pattern. The map at the top (right) is a part of the texture measured on road surface A'. The map at the bottom is the resulting combined roughness. The sampling interval used for the input data was chosen to be 1 mm to avoid excessive time consuming 3D envelopment calculations.

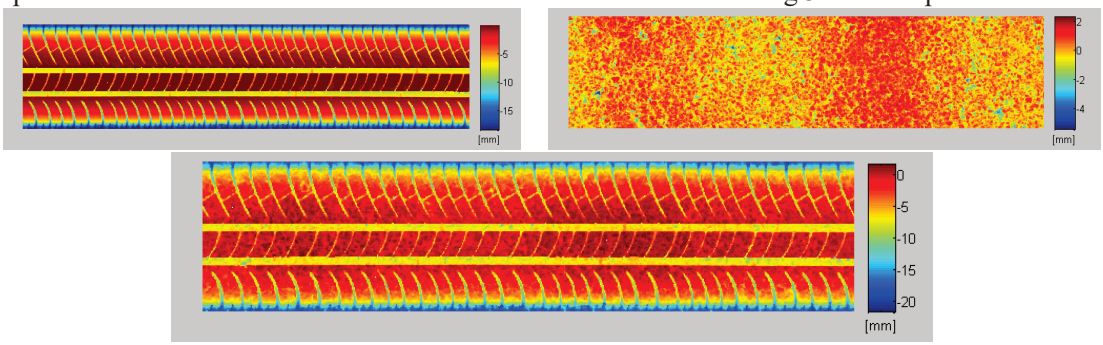

Figure 10 – Top left: tyre tread pattern – Top right: road roughness – Bottom: combined tyre/road roughness

5.2 3D Envelopment Principle

Calculating static contact as described in section 4.3 requires significant computing resources. It is inconceivable to perform such a calculation in a prediction tool over the entire width of the tyre and along a substantial length such as for the 2D enveloped profiles (1.50 m) or even over the length of the tyre contact area. The proposed method for the 3D envelopment is to evaluate the contact between the combined tyre/road roughness on the entire width of the tyre, but over a reduced length in the rolling direction while ensuring that the achieved result is identical or very close to the result over a greater length. A length of 25 mm was found satisfactory for a passenger car tyre. The envelopment is thus obtained by considering an elastic solid of length 25 mm and of tyre width, which is moved in the rolling direction along the entire length of the tyre/road sample. For each position of the sliding block, a static contact calculation is performed. The problem is considered semi-periodic in the rolling direction in order to avoid edge effects in this direction. It is not necessary to make the problem periodic in the transverse direction due to the curved tyre transverse shape. Once the contact evaluated, the transverse profile in the middle of the block is saved. The final 3D enveloped roughness is made of the juxtaposition of the saved transverse profiles for the successive positions of the sliding block. The method is illustrated Figure 11. The 3D enveloped surface obtained from the combined roughness shown Figure 10 is drawn in Figure 12 together with the pressure map obtained at the same time.

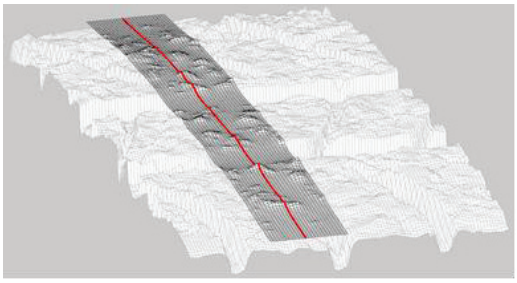

Figure 11 – Loaded sliding rubber block (in black) moving over the combined tyre/road roughness (in white) and selected transverse profile (in red)

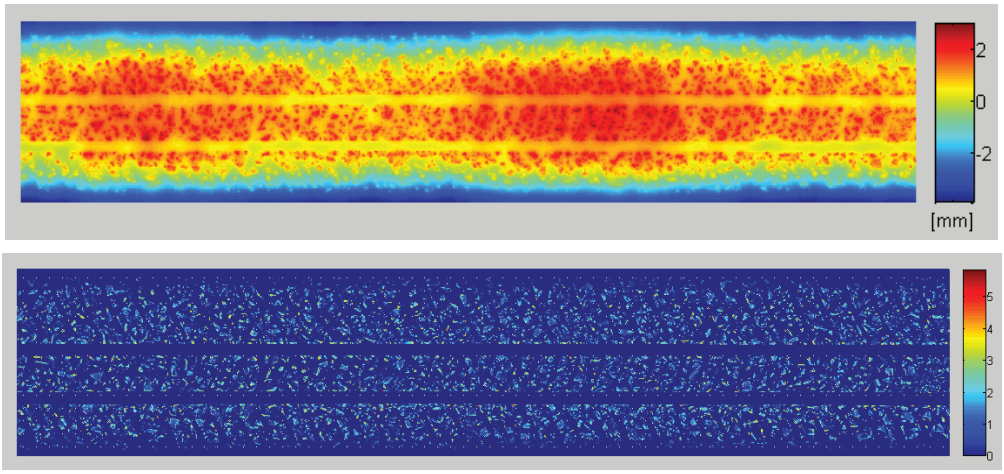

Figure 12 – Top: enveloped tyre/road combined roughness –Bottom: pressure map

5.3 Output Data

The output of the 3D envelopment procedure consists of longitudinal profiles extracted from the resulting enveloped surface. The position of these profiles is selected with the help of the transverse pressure distribution averaged over the longitudinal direction. Two examples of averaged pressure transverse distribution are given Figure 13, the red one obtained for the patterned E3A tyre, the black one obtained for a slick tyre with the same overall transverse shape. In this case, eight profiles are extracted, distributed at constant interval for the slick tyre, avoiding the longitudinal grooves for the patterned tyre, between the lateral positions of 0.03 m to 0.017 m. Examples of 1 m long extracted profiles are shown Figure 14.

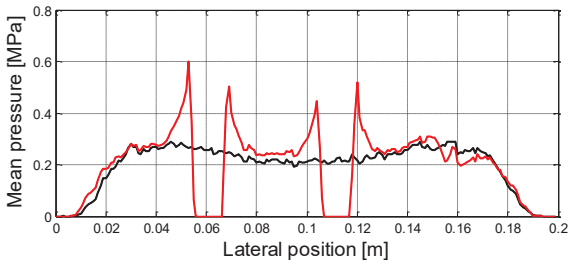

Figure 13 – Contact pressure averaged over the rolling direction - Red curve: patterned E3A tyre – Black curve: slick tyre

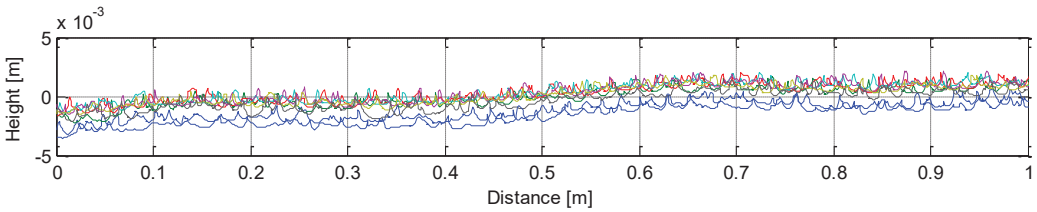

Figure 14 – Examples of longitudinal profiles extracted from the enveloped surface

Enveloped tyre/road roughness levels are evaluated from the extracted profiles. The enveloped roughness levels obtained for a Young's modulus value $E = 4$ MPa are given in Figure 15 for all the road surfaces previously used for calibrating the 2D model. The spectrum obtained for a perfectly smooth road surface and the patterned tyre is added as a dashed black curve. Enveloped spectra obtained with the tyre without grooves exhibit a significant spread, greater than 20 dB for certain frequencies. The lowest levels are those obtained for the ISO surface, the highest are those of surface A'. For the patterned tyre, the spread is significantly reduced at frequencies corresponding to the tread blocks scrolling. Two peaks are to be noticed at 1 kHz and 2 kHz corresponding to wavelengths of 25 mm and 12.5 mm given the rolling speed of 90 km/h. The combined roughness spectra are more or less

affected around these frequencies. The levels of the ISO surface are mostly influenced even at frequencies below 500 Hz, while those of surface A' are almost unchanged.

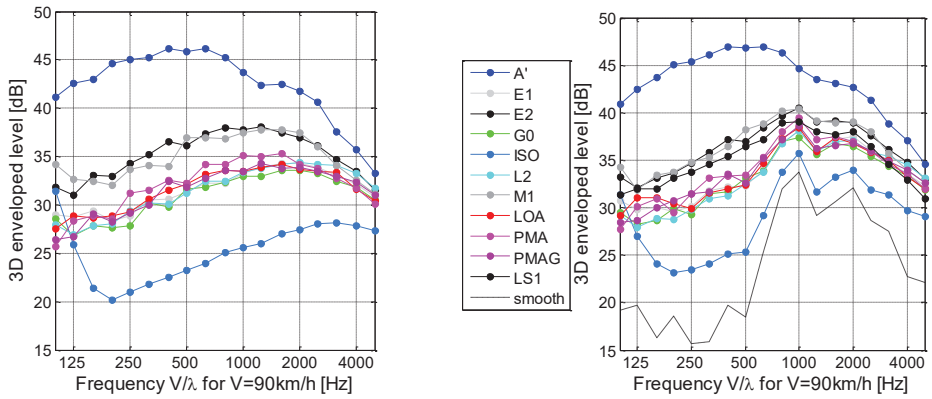

Figure 15 – 3D combined enveloped roughness levels as a function of time frequency for V=90 km/h – Left: slick tyre – Right: patterned tyre

6. MODEL FITTING AND RESULTS

The enveloped combined tyre/road roughness levels have been evaluated for four values of E: 1, 2, 4 and 8 MPa. The first three values gave almost the same results. For the fourth value, the results were slightly degraded. Here, the results are presented for $E = 4$ MPa.

6.1 Correlations between 3D Enveloped Texture Levels and Noise Levels

The maps drawn in Figure 16 show the correlation coefficient values obtained between measured third-octave band noise levels with the patterned E3A tyre and third-octave band enveloped roughness levels for frequency pairs $(f_i, V/\lambda_j)$, ranging from 100 Hz to 5 kHz, for all 11 non-absorbent road surfaces used for the calibration of the 2D model. The diagonal of the maps stands for the equality between noise frequency and roughness passing frequency (V=90km/h). The map on the left is obtained with the 2D road texture envelopment while the map on the right is obtained with the 3D tyre/road roughness envelopment. On both maps, good correlations are observed between 250 Hz and 1250 Hz, the latter frequency corresponding to the transition frequency f_t already identified. Beyond this frequency, very poor correlations are observed. It is to be noticed that the correlations in low and medium frequency ranges with the 3D combined tyre/road roughness envelopment are improved with respect to those obtained with the 2D road texture envelopment. The area where best correlations are observed is extended and shifted to higher roughness passing frequencies. The consequences regarding global CB noise level prediction are given in the next paragraph.

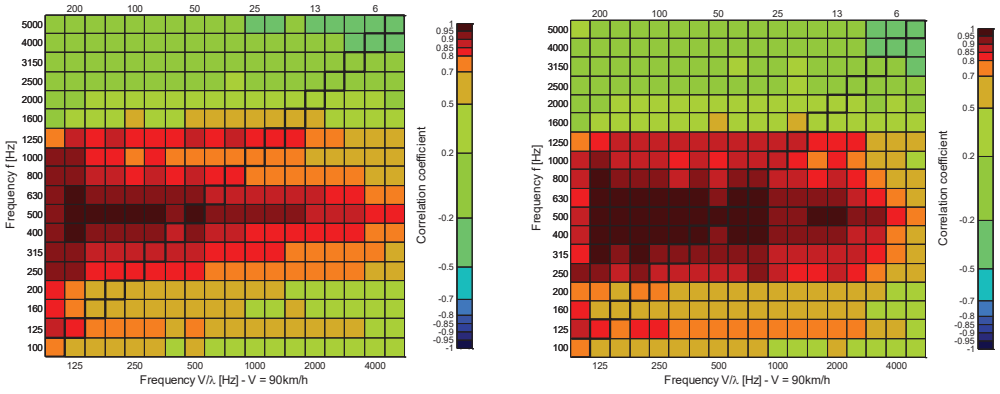

Figure 16 - Maps of correlation coefficients evaluated between third-octave enveloped texture levels and CB noise levels – Left : 2D enveloped road texture – Right : 3D enveloped combined tyre/road roughness

6.2 Prediction of CB Noise Levels of Dense Surfaces

The HyRoNE model based on the 3D tyre/road roughness envelopment instead of the 2D road texture envelopment has been constructed. In the high frequency range, as for the 2D version, raw texture levels have been used. The relationship between measured and predicted global CB noise levels at 90 km/h for the patterned E3A tyre is given in Figure 17. It is to be compared with the graph on the right of Figure 4. The prediction error made over the 11 road surfaces amounts to 0.7 dBA in average, while the error obtained with the 2D texture envelopment amounts to 1.0 dBA. The improvement is mainly due to the reduction of the errors made on the ISO surface and on surface A'.

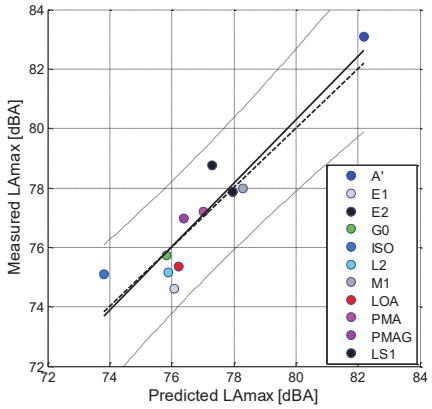

Figure 17 – Relationship between predicted and measured LAmax at 90 km/h reconstructed from third-octave CB levels

The errors made on the third-octave CB levels are drawn Figure 18. They do not exceed 3 dB in absolute value. To improve global noise level prediction, these errors should be reduced. The separation of main generation mechanisms over a common frequency range around the transition frequency, as described in (1), was given a try to reduce these errors but it was not successful. More advanced texture related quantities such as those used in the SPERoN model (5) for the prediction of air-pumping contributions and the physical background on air-pumping sources provided by CFD simulations within the framework of the project (11,12) will probably be helpful to perform this separation.

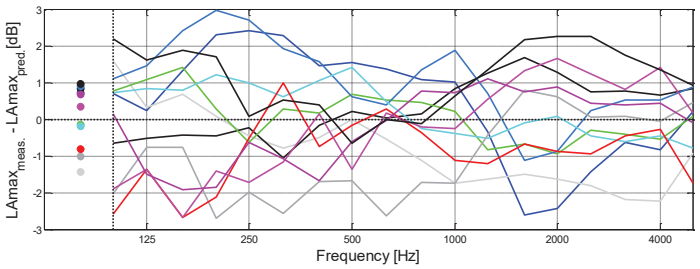

Figure 18 – Prediction errors on third-octave CB levels at 90 km/h

7. CONCLUSION

The HyRoNE model has been constructed on a set of conventional non-absorbent road surfaces which are parts of a database including 3D texture, rolling noise and absorption measurements collected within the DEUFRAKO ODSURF project in France and in Germany. The fitting of the version based on 2D texture profiles has shown the trends obtained on smooth road surfaces such as an ISO surface but also the difficulty to handle such smooth surfaces.

The availability of 3D road textures and the tread pattern of the tyre used in the experiments enabled to use a combined tyre/road roughness to address this difficulty. A new 3D envelopment procedure was developed for the prediction of the noise radiated by the tyre belt. It is based on a 3D contact model between a rigid body and an elastic half-space.

This 3D envelopment procedure has been tested and shown to improve the HyRoNE predictions

with respect to the 2D road profile envelopment when a smooth road surface is taken into account. However further reliable improvements have to be sought on texture related quantities for air-pumping noise prediction to be able to consider separate contributions of both main generation mechanisms over the whole frequency range.

ACKNOWLEDGEMENTS

This research was funded by the French ADEME within the framework of the DEUFRAKO ODSURF project and by the French Labex CeLyA. The authors are also grateful to the French and German partners, especially to BASt and Müller-BBM, for making the measurements in Germany possible and easier.

REFERENCES

1. Sandberg U, Descornet G. Road surface influence on tire/road noise – Part 1 & Part 2. Proc INTER-NOISE 1980; 8-10 December 2015; Miami, Florida 1980.
2. Cesbron J, Gary V, Klein P, Clairet JM. On site characterization of optimized very thin asphalt concrete. Proc EURO-NOISE 2015; 31 May-3 June 2015; Maastricht, the Netherlands 2015.
3. Cesbron J, Klein P, Une nouvelle base de données texture/bruit pour la prévision du bruit de contact pneumatique/chaussée. Proc CFA/VISHNO 2016; 11-15 April 2016; Le Mans, France 2016 (in French).
4. Klein P, Hamet JF. Tyre/road noise prediction with the HyRoNE model. Proc INTER-NOISE 2007; 28-31 August 2007; Istanbul, Turkey 2007.
5. Beckenbauer T, Klein P, Hamet JF, Kropp W. Tyre/road noise prediction: a comparison between the SPERoN and HyRoNE models – Part 1. Proc Acoustics'08; 29 June-4 July 2008; Paris, France 2008.
6. Klein P, Beckenbauer T, Hamet JF, Kropp W. Tyre/road noise prediction: a comparison between the SPERoN and HyRoNE models – Part 2. Proc Acoustics'08; 29 June-4 July 2008; Paris, France 2008.
7. Sandberg U, Ejsmont JA. Tyre/road noise reference book. INFORMEX 2002.
8. Klein P, Hamet JF, Anfosso-Lédée F. An envelopment procedure for tire/road contact. Proc SURF 2004; 6-10 June 2004; Toronto, Canada 2004.
9. Klein P. Influence du revêtement routier sur le bruit de roulement: le modèle HyRoNE. Proc CFA 2010; 12-16 April 2010; Lyon, France 2010 (in French).
10. Dubois G, Cesbron J, Yin HP, Anfosso-Lédée F. Numerical evaluation of tyre/road contact pressures using a multi-asperity approach. International Journal of Mechanical Sciences 2012;54(1):84-94.
11. Conte F, Klein P. 3D CFD modelling of air-pumping noise from road cavities with constant volume. Proc INTER-NOISE 2013; 15-18 September 2013; Innsbrück, Austria 2013.
12. Conte F, Klein P. Investigating lateral porosity effect on air pumping noise from connected road cavities with CFD simulations. Proc INTER-NOISE 2014; 16-19 November 2014; Melbourne, Australia 2014.